Three-Dimensional Neutronics and Photonics Analysis for PBFA-II

M.E. Sawan

February 1984

UWFDM-570

FUSION TECHNOLOGY INSTITUTE

UNIVERSITY OF WISCONSIN

MADISON WISCONSIN

DISCLAIMER

This report was prepared as an account of work sponsored by an agency of the United States Government. Neither the United States Government, nor any agency thereof, nor any of their employees, makes any warranty, express or implied, or assumes any legal liability or responsibility for the accuracy, completeness, or usefulness of any information, apparatus, product, or process disclosed, or represents that its use would not infringe privately owned rights. Reference herein to any specific commercial product, process, or service by trade name, trademark, manufacturer, or otherwise, does not necessarily constitute or imply its endorsement, recommendation, or favoring by the United States Government or any agency thereof. The views and opinions of authors expressed herein do not necessarily state or reflect those of the United States Government or any agency thereof.

Three-Dimensional Neutronics and Photonics Analysis for PBFA-II

M.E. Sawan

Fusion Technology Institute
University of Wisconsin
1500 Engineering Drive
Madison, WI 53706

http://fti.neep.wisc.edu

February 1984

UWFDM-570

THREE-DIMENSIONAL NEUTRONICS AND PHOTONICS ANALYSIS FOR PBFA-II

Mohamed E. Sawan

Fusion Engineering Program
Nuclear Engineering Department
University of Wisconsin
Madison, Wisconsin 53706

February 1984

UWFDM-570

I. Introduction

The Particle Beam Fusion Accelerator (PBFA-II)[1] under development at Sandia National Laboratories is expected to come on line by 1986. Targets are to be ignited in the facility producing 2.45 MeV D-D fusion neutrons and 14.1 MeV D-T fusion neutrons. 10^{14} D-D neutrons and 10^{17} D-T neutrons are expected to be produced in each shot. These neutrons produced at the center of the target chamber could penetrate into the basement and damage the laser triggering systems and other sensitive diagnostic equipment. In this report three-dimensional coupled neutronics-photonics calculations are described for PBFA-II. Neutron and gamma fluxes and spectra are given at different locations in the basement. Results are given for both D-D and D-T fusion. The results are useful in determining the absorbed radiation dose in the sensitive equipment and will help determine the best configuration of the laser triggering systems and other diagnostic equipment.

II. Calculational Model

Three-dimensional neutronics and photonics calculations have been performed using the multi-group Monte Carlo code MORSE.[2] A coupled 25 neutron - 21 gamma group cross section library was used. The library was obtained by collapsing the 171 neutron - 36 gamma group cross section VITAMIN-C library[3] based on the ENDF/B-IV cross section evaluation. Tables 1 and 2 give the boundaries for the neutron and gamma energy groups used in the calculations.

The combinatorial geometry capability of the MORSE code was used to model the problem geometry. The upper shield tank, the target cavity, the accelerator tank and the basement area with surrounding concrete and soil were included in the model. Volume detectors were used to calculate the neutron and gamma fluxes and spectra at the proposed locations of the sensitive

Table 1. Neutron 25 Group Structure in eV

Group Limits

Group	E(Top)	E(Low)	E(Mid Point)
1	1.4918 (+7)	1.3499 (+7)	1.4208 (+7)
2	1.3499 (+7)	1.2214 (+7)	1.2856 (+7)
3	1.2214 (+7)	1.1052 (+7)	1.1633 (+7)
4	1.1052 (+7)	1.0000 (+7)	1.0526 (+7)
5	1.0000 (+7)	9.0484 (+6)	9.5242 (+6)
6	9.0484 (+6)	8.1873 (+6)	8.6178 (+6)
7	8.1873 (+6)	7.4082 (+6)	7.7979 (+6)
8	7.4082 (+6)	6.7032 (+6)	7.0557 (+6)
9	6.7032 (+6)	6.0653 (+6)	6.3843 (+6)
10	6.0653 (+6)	5.4881 (+6)	5.7787 (+6)
11	5.4881 (+6)	4.4933 (+6)	4.9907 (+6)
12	4.4933 (+6)	3.6788 (+6)	4.0860 (+6)
13	3.6788 (+6)	3.0119 (+6)	3.3453 (+6)
14	3.0119 (+6)	2.4660 (+6)	2.7390 (+6)
15	2.4660 (+6)	1.3534 (+6)	1.9097 (+6)
16	1.3534 (+6)	7.4274 (+5)	1.0481 (+6)
17	7.4274 (+5)	4.0762 (+5)	5.7518 (+5)
18	4.0762 (+5)	1.6573 (+5)	2.8667 (+5)
19	1.6573 (+5)	3.1828 (+4)	9.8779 (+4)
20	3.1828 (+4)	3.3546 (+3)	1.7591 (+4)
21	3.3546 (+3)	3.5358 (+2)	1.8541 (+3)
22	3.5358 (+2)	3.7267 (+1)	1.9542 (+2)
23	3.7267 (+1)	3.9279 (+0)	2.0597 (+1)
24	3.9279 (+0)	4.1399 (-1)	2.1718 (+0)
25	4.1399 (-1)	2.200 (-2)	2.1800 (-1)

Table 2. Gamma-Ray Energy Group Structure in MeV

Group Limits

Group	E(Top)	E(Low)	E(Mid Point)
1	14.00	12.00	13.00
2	12.00	10.00	11.00
3	10.00	8.00	9.00
4	8.00	7.50	7.75
5	7.50	7.00	7.25
6	7.00	6.50	6.75
7	6.50	6.00	6.25
8	6.00	5.50	5.75
9	5.50	5.00	5.25
10	5.00	4.50	4.75
11	4.50	4.00	4.25
12	4.00	3.50	3.75
13	3.50	3.00	3.25
14	3.00	2.50	2.75
15	2.50	2.00	2.25
16	2.00	1.50	1.75
17	1.50	1.00	1.25
18	1.00	0.40	0.70
19	0.40	0.20	0.30
20	0.20	0.10	0.15
21	0.10	0.01	0.055

equipment in the basement. A vertical cross section of the geometrical model used in the calculations is given in Fig. 1. Plan views at different elevations above the basement floor, corresponding to Z = -3.5, -4.7, and -6 m, are shown in Figs. 2, 3, and 4. Because of symmetry only one-fourth of the PBFA-II system was modeled with reflecting surfaces used at the planes of symmetry Y = 0 and X = 0.

Zones 1-5 shown in Fig. 4 have been used to represent possible locations for the YAG lasers. Zones 6 and 7 represent possible locations for the KrF laser and splitter table, respectively. Each of these volume detectors has a volume of 3.6×10^5 cm^3. These zones are 1 m above the basement floor which is the nominal elevation of the laser triggering systems in PBFA-II. The neutron and gamma fluxes have been calculated also at zones 8, 9, and 10 located 2.3 m above the basement floor and zones 11, 12, and 13 located 3.5 m above the basement floor to investigate the effect of raising the laser triggering systems further above the basement floor. Zone 14 represents the air environment in the basement. Air at 20°C and 660 torr was considered to occupy zones 1-14.

Zone 15 represents the concrete walls and base for the basement. The walls are 40 cm thick and two layers of concrete base for the basement that are 20 and 90 cm thick are used as shown in Fig. 1. Hanford ordinary concrete at a density of 2.258 g/cm^3 was used in zone 15. Zone 16 represents the 1.1 cm stainless steel floor of the accelerator tank. Zone 17 corresponds to the 2.5 cm thick stainless steel floor for the target cavity. Zone 18 represents the 1.25 cm thick stainless steel elevator floor. Type 304 stainless steel was used in zones 16, 17, and 18. Zone 19 represents the soil surrounding the basement. A minimum thickness of 90 cm was maintained behind the concrete

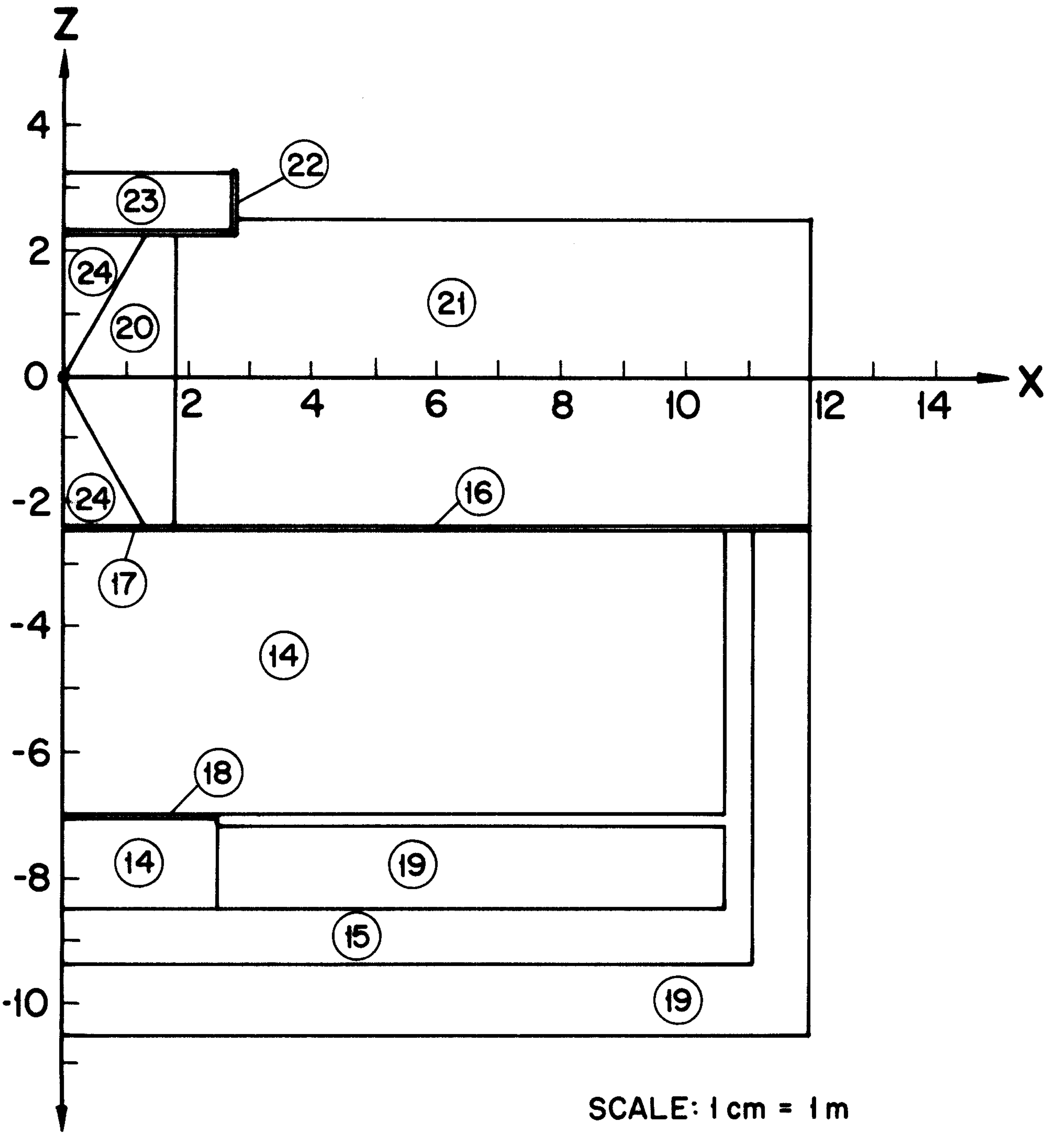

Fig. 1. Vertical cross section of the geometrical model.

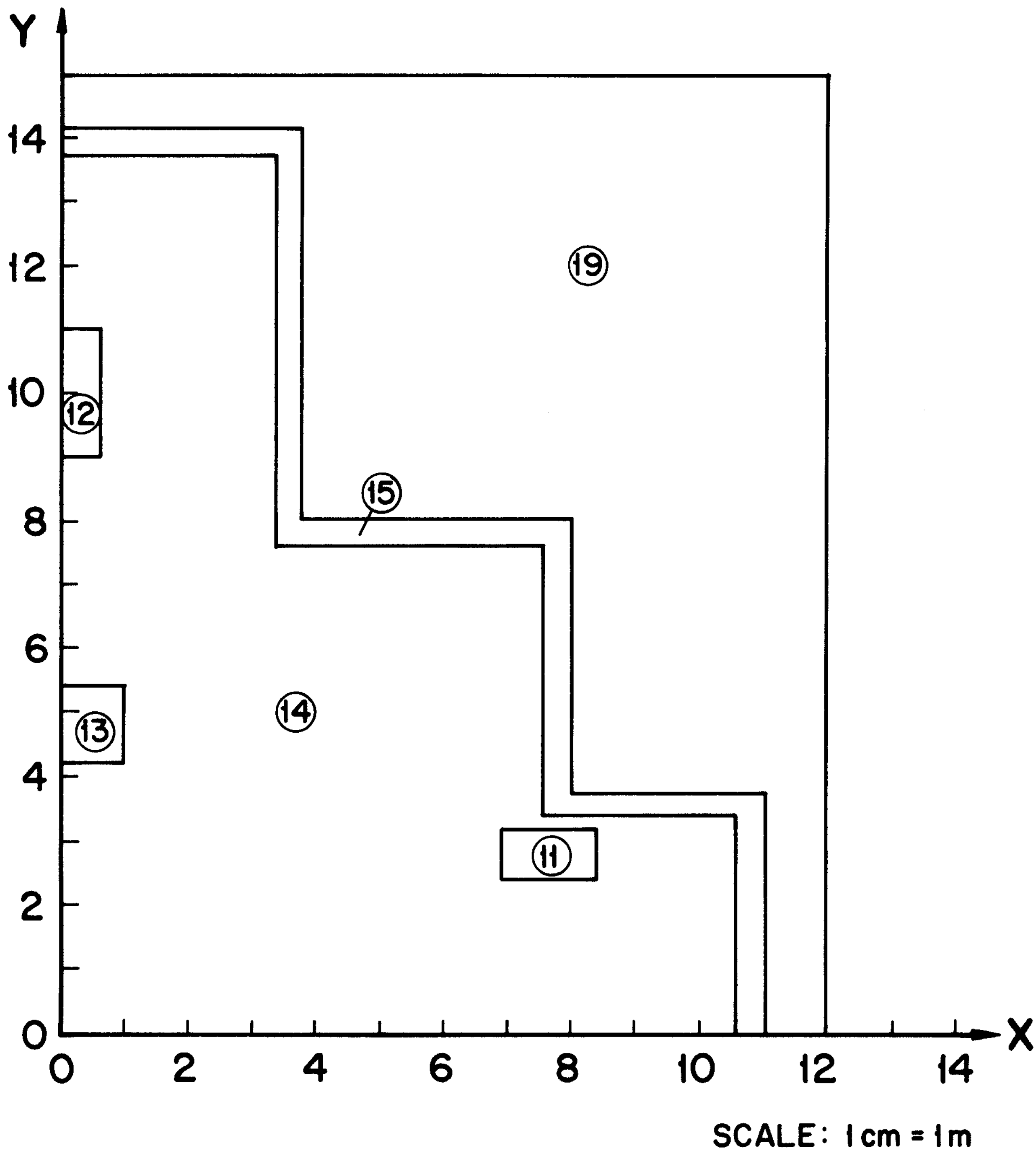

Fig. 2. Horizontal cross section at 3.5 m above basement floor.

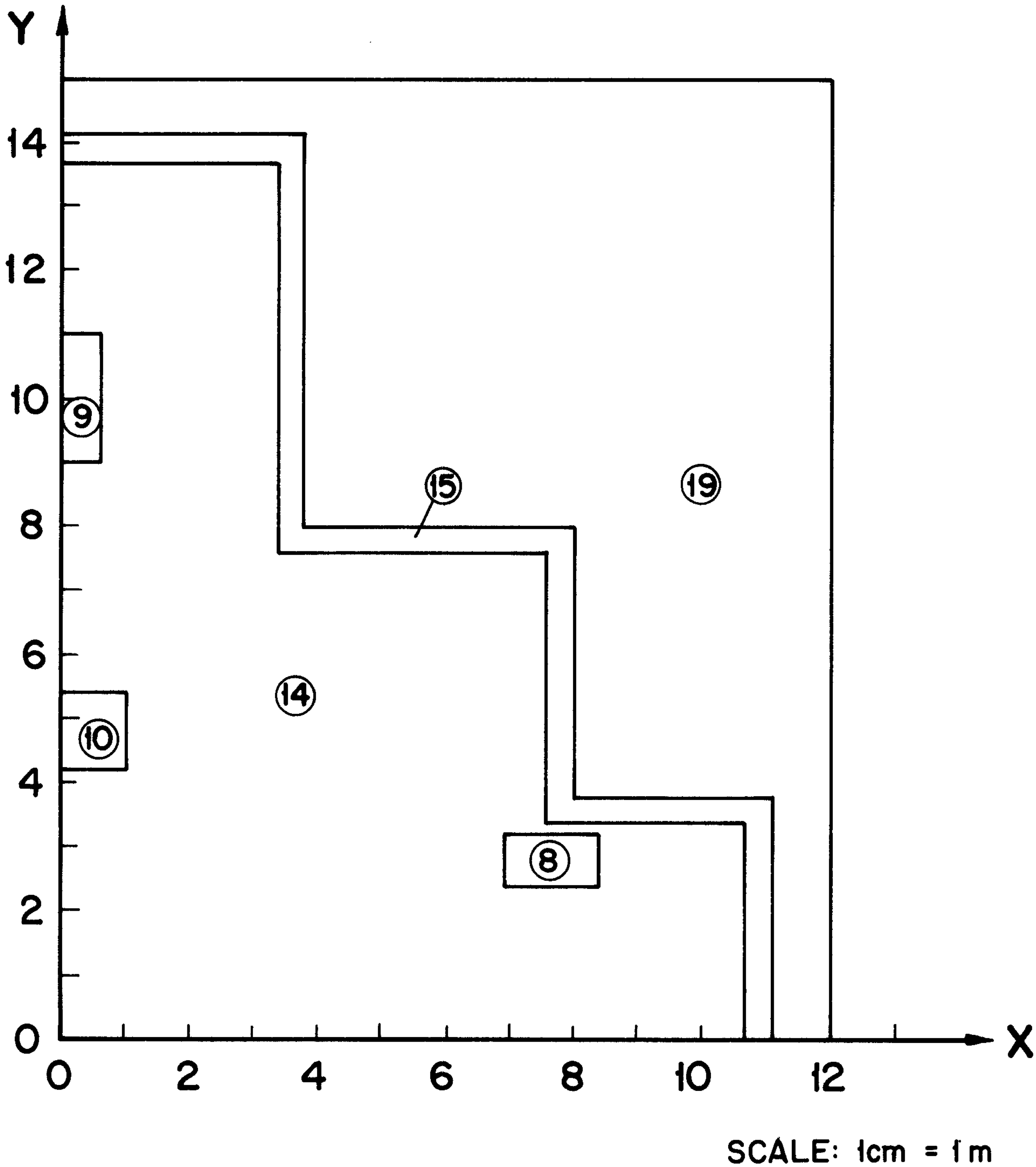

Fig. 3. Horizontal cross section at 2.3 m above basement floor.

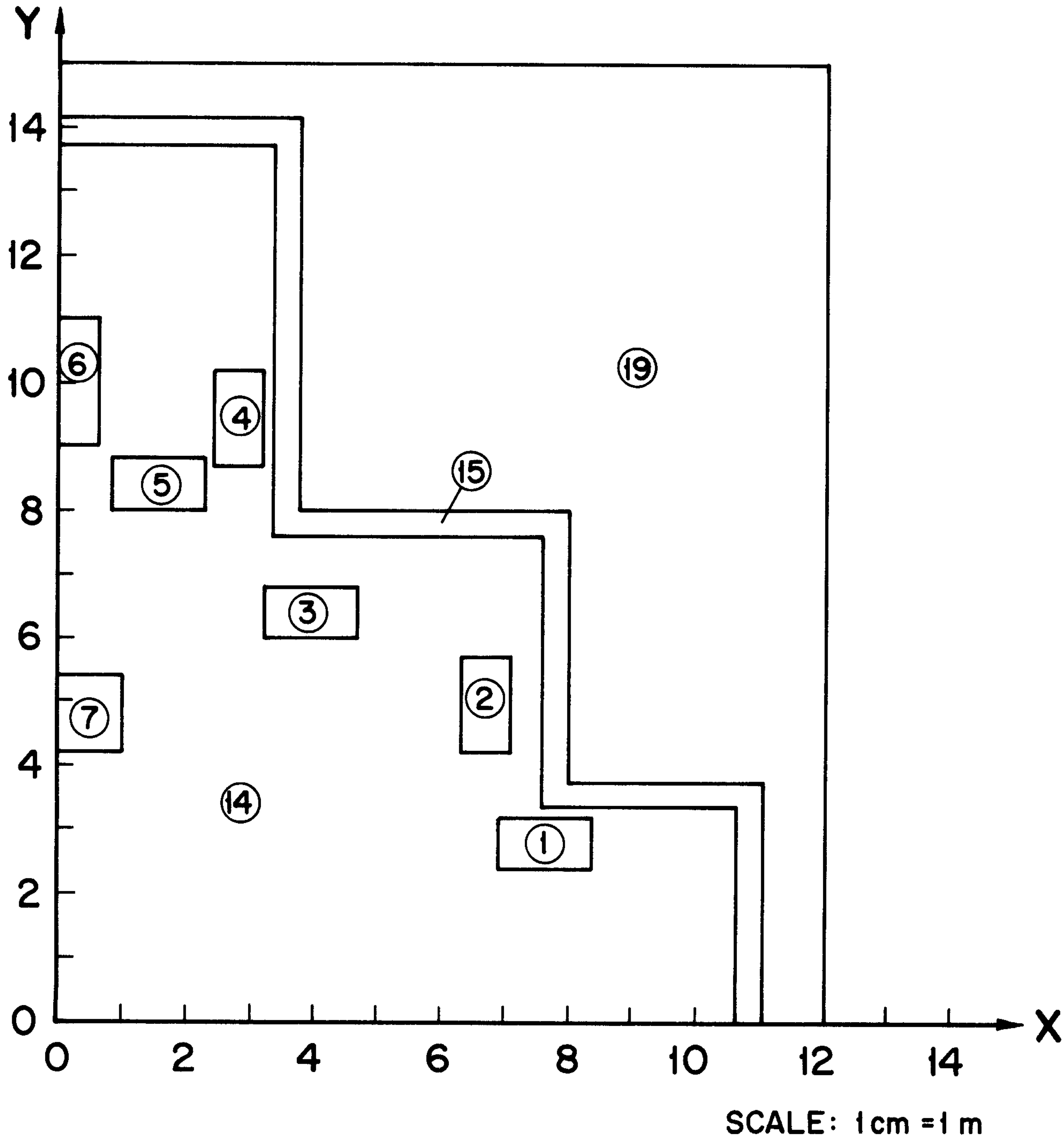

Fig. 4. Horizontal cross section at 1 m above basement floor.

walls and base to properly account for any backscattered neutrons or gamma photons. The soil was considered to consist of 90 wt % SiO_2 and 10 wt % H_2O.

Zone 20 is representative of the aluminum transmission line section of the target chamber. The transmission lines occupy 3% of the volume of this zone. Zone 21 is the accelerator tank that consists of 3 vol % Al and 97 vol % H_2O. Zone 22 corresponds to the 10 cm thick 304 SS shield tank wall and floor. Zone 23 represents the water in the shield tank. Zone 24 consists of two cones with a common vertex at the target. No material exists in these cones. Table 3 gives the composition and density for the materials used in this analysis.

An isotropic point neutron source, representative of the neutrons emerging from the fusion reactions in the target, is located at the center of the target cavity. Two calculations have been performed for D-T and D-D fusion neutrons. The 14.1 MeV D-T fusion neutron is emitted in energy group 1, while the 2.45 MeV D-D fusion neutron originates in group 15. In order to get statistically adequate estimates for the flux in the zones representative of the locations of the laser triggering systems in the basement, an angular source biasing technique was used. The biasing technique is similar to that used previously for the radiation shielding analysis of the final focusing magnets of HIBALL.(4) The direction of the source neutron is picked from a biased distribution function that forces 90% of the source neutrons to impinge on the stainless steel floor of the target chamber with the enhanced chance of going into the basement. For the final results to be unbiased, the statistical weight of the source was modified by the ratio of the unbiased (isotropic) and biased distribution functions at the selected direction. Forty thousand histories were used in each Monte Carlo calculation yielding statistical

Table 3. Composition and Atomic Density for Materials Used in the Analysis

Zone	Material	Density (g/cm^3)		Nuclide Density (nuclei/b·cm)
1-14	Air	1.046×10^{-3}	N	3.3956×10^{-5}
			O	0.1400×10^{-6}
			A	2.0920×10^{-7}
15	Ordinary concrete	2.258	H	0.00418
			O	0.63855
			Si	0.01567
			Ca	0.00481
			Fe	0.00195
16-18, 22	Type 304 SS	7.93	Fe	0.06331
			Cr	0.01654
			Ni	0.00651
19	Soil	1.8	H	0.01206
			O	0.03851
			Si	0.01624
20	3 vol % Al	2.699	Al	1.808×10^{-3}
	97 vol % void	0		
21	3 vol % Al	2.699	Al	1.808×10^{-3}
	97 vol % H_2O	1	H	6.488×10^{-2}
			O	3.244×10^{-2}
23	Water	1	H	6.689×10^{-2}
			O	3.344×10^{-2}
24	Void	0		

uncertainties less than ~ 20% in the calculated neutron and gamma fluxes in zones 1 to 13 which represent possible locations for the laser triggering systems.

III. Results and Discussion

Table 4 gives the total neutron and gamma fluxes in the zones representative of the possible locations of the laser triggering systems. These results are given for the case of a D-T fusion and are normalized to one 14.1 MeV fusion neutron. The results are accurate to within 10-20%. Zone 7 has the largest neutron and gamma fluxes. This is primarily due to the fact that among the different detector zones at 1 m above the basement floor, zone 7 is the closest to the target (smallest radius). Comparing the results for zones 7, 10, and 13, we notice that both the neutron and gamma fluxes decrease as the elevation above the basement floor increases. This results from the additional shielding provided by the accelerator tank (zone 21). Zone 7 is protected from the direct line of sight of source neutrons only by the thin steel floor of the target chamber.

The neutron spectra in zones 1, 6, 7, and 10 are given in Table 5. While the total flux is accurate to within 10-20%, the flux in each energy group can be different by up to a factor of two. However, the general shape of the spectrum in the different zones is satisfactorily represented by the results. The fractions of neutrons in different energy ranges for these zones are given in Table 6. The gamma spectra in these zones are given in Table 7. The results indicate that for the same radius, the spectrum softens as the elevation above the basement floor is increased. This is attributed to the additional shielding of the water in the accelerator tank. This effect can be seen by comparing the spectra in zones 7 and 10. Raising the splitter table will,

Table 4. Total Neutron and Gamma Fluxes in Different Zones

(10^{-7} particles/cm^2/D-T fusion)

Zone	Neutron	Gamma
1	3.133	2.275
2	3.903	2.997
3	4.092	2.900
4	2.210	1.367
5	2.922	2.107
6	2.074	1.416
7	9.722	6.722
8	3.033	2.666
9	1.944	1.690
10	7.033	4.930
11	3.408	2.232
12	2.111	1.560
13	5.936	4.689

Table 5. Neutron Spectra in Different Zones

$(n/cm^2/D\text{-}T\ fusion/group)$

Energy Group	Zone 1	Zone 6	Zone 7	Zone 10
1	3.556 E-10	0	2.283 E-7	3.419 E-8
2	2.583 E-10	3.264 E-10	6.104 E-9	2.988 E-9
3	4.181 E-10	4.865 E-10	1.467 E-8	2.405 E-9
4	3.479 E-9	3.326 E-10	6.538 E-10	1.983 E-9
5	4.459 E-11	2.903 E-10	6.059 E-10	2.938 E-10
6	3.639 E-9	2.007 E-11	8.078 E-10	8.396 E-10
7	8.799 E-10	3.333 E-10	5.688 E-10	3.307 E-10
8	4.319 E-10	0	7.313 E-10	1.363 E-8
9	1.069 E-9	0	1.428 E-9	5.522 E-9
10	1.144 E-10	2.486 E-9	1.411 E-9	1.853 E-9
11	9.771 E-10	1.908 E-10	7.581 E-9	4.817 E-9
12	9.250 E-10	6.431 E-10	1.115 E-8	2.051 E-9
13	2.638 E-9	1.231 E-9	9.651 E-9	5.257 E-9
14	2.415 E-9	1.455 E-9	7.943 E-8	2.481 E-8
15	2.859 E-8	3.256 E-9	5.062 E-8	5.688 E-8
16	4.814 E-8	1.458 E-8	6.611 E-8	7.389 E-8
17	7.691 E-9	1.696 E-8	1.535 E-8	2.230 E-8
18	2.336 E-8	1.987 E-8	3.911 E-8	3.214 E-8
19	1.254 E-8	6.382 E-9	5.903 E-8	3.884 E-8
20	2.069 E-8	4.552 E-9	3.569 E-8	4.128 E-8
21	1.083 E-8	1.933 E-8	1.724 E-8	1.764 E-8
22	2.630 E-8	7.639 E-9	8.140 E-8	8.890 E-8
23	2.617 E-8	3.078 E-8	5.665 E-8	3.800 E-8
24	1.493 E-8	2.050 E-8	6.417 E-8	6.836 E-8
25	7.639 E-8	5.577 E-8	1.236 E-7	1.242 E-7
TOTAL	3.133 E-7	2.075 E-7	9.722 E-7	7.033 E-7

Table 6. Fractions of Neutrons in Different Energy Ranges for a D-T Fusion Neutron Source

	Zone 1	Zone 6	Zone 7	Zone 10
Group 1 (13.5 < E < 15 MeV)	0.1%	0%	23%	5%
Group 25 (thermal neutrons)	24%	27%	13%	18%
Groups 16-25 (E < 1.35 Mev)	85%	95%	58%	78%

Table 7. Gamma Spectra in Different Zones

(γ/cm^2/D-T fusion/group)

Energy Group	Zone 1	Zone 6	Zone 7	Zone 10
1	0	0	0	0
2	0	0	2.287 E-9	0
3	6.517 E-9	6.625 E-11	5.246 E-8	6.492 E-9
4	4.820 E-9	1.307 E-9	8.225 E-9	9.635 E-9
5	2.713 E-9	2.917 E-10	4.764 E-8	4.303 E-9
6	2.104 E-10	9.194 E-10	3.007 E-9	8.174 E-9
7	2.363 E-9	1.858 E-9	5.167 E-9	5.615 E-9
8	1.133 E-9	6.243 E-10	5.067 E-9	3.981 E-9
9	5.174 E-10	8.659 E-10	4.763 E-9	2.692 E-9
10	2.595 E-9	3.910 E-10	4.384 E-8	6.056 E-9
11	1.007 E-9	7.352 E-10	7.833 E-9	4.531 E-9
12	1.888 E-9	1.114 E-9	6.024 E-9	2.145 E-8
13	2.298 E-9	3.556 E-9	5.444 E-9	7.583 E-9
14	2.330 E-9	4.185 E-9	1.086 E-8	8.590 E-9
15	1.548 E-8	3.815 E-9	3.176 E-8	1.873 E-8
16	5.816 E-9	2.224 E-9	2.718 E-8	1.721 E-8
17	6.271 E-9	8.667 E-9	2.132 E-8	2.742 E-8
18	4.800 E-8	3.981 E-8	1.474 E-7	1.256 E-7
19	6.548 E-8	3.259 E-8	1.170 E-7	1.165 E-7
20	5.708 E-8	3.349 E-8	1.219 E-7	1.008 E-7
21	1.055 E-9	4.239 E-9	2.935 E-9	1.007 E-9
TOTAL	2.275 E-7	1.416 E-7	6.722 E-7	4.930 E-7
Fraction in Groups 18-21 (E < 1 MeV)	76%	78%	58%	70%

therefore, help reduce the high energy component of the spectrum considerably. Softer spectra are obtained by increasing the radius for the same elevation as shown by comparing the spectra in zones 6, 1, and 7. More than 85% of the neutrons have energies below 1.35 MeV for all proposed locations of the YAG and KrF lasers. More than 70% of the gamma photons have energies below 1 MeV at these locations.

The total neutron and gamma fluxes in the different zones are given in Table 8, with the results being normalized to one 2.45 MeV D-D fusion neutron. The uncertainty in the gamma flux is larger than in the D-T case due to the fewer gamma tracks generated by the lower energy neutrons. A comparison between the total neutron fluxes obtained in the different zones from D-T and D-D fusion neutrons is shown in Fig. 5. The results for the total gamma flux are illustrated in Fig. 6. Spatial variations of the total neutron and gamma fluxes are similar to those obtained in the D-T fusion case. In general, the neutron flux in the D-D fusion case is larger than that in the D-T case because of the lower absorption probability in the water accelerator tank at the D-D neutron energy. Larger absorption at the D-T neutron energy is attributed to (n,α) and (n,p) reactions with O and Al. The neutron flux in zone 7 which is shielded only by 304 SS, is lower than that in the D-T case due to the absence of neutron multiplication via the (n,2n) reactions in steel. The total gamma flux is lower than that in the D-T case because of less gamma production by the lower energy neutrons.

The neutron and gamma spectra in zones 1, 6, 7, and 10 are given in Tables 9 and 10, respectively. The neutron spectrum is much softer than the D-T case because of the lower source neutron energy. A relatively large fraction of the neutrons remains in the source group (group 15) because of its

Table 8. Total Neutron and Gamma Fluxes in Different Zones

(10^{-7} particles/cm^2/D-D fusion)

Zone Number	Neutron	Gamma
1	4.214	1.756
2	3.797	1.916
3	4.133	1.736
4	3.026	1.247
5	3.538	1.486
6	2.460	1.522
7	8.340	6.165
8	4.906	1.423
9	2.957	1.371
10	8.583	3.762
11	3.944	1.287
12	2.095	1.108
13	6.613	3.106

Table 9. Neutron Spectra in Different Zones

(n/cm^2/D-D fusion/group)

Energy Group	Zone 1	Zone 6	Zone 7	Zone 10
15	2.639 E-8	1.335 E-8	1.944 E-7	9.764 E-8
16	5.333 E-8	4.847 E-8	1.028 E-7	1.195 E-7
17	2.035 E-8	1.958 E-9	3.264 E-8	2.810 E-8
18	2.771 E-8	1.322 E-8	5.694 E-8	4.444 E-8
19	4.243 E-8	1.813 E-8	4.472 E-8	1.549 E-7
20	3.133 E-8	2.542 E-8	3.410 E-8	3.806 E-8
21	4.785 E-8	1.088 E-8	7.431 E-8	6.417 E-8
22	2.590 E-8	1.772 E-8	3.861 E-8	4.181 E-8
23	2.646 E-8	1.390 E-8	3.319 E-8	4.674 E-8
24	2.333 E-8	6.958 E-9	4.882 E-8	5.368 E-8
25	9.639 E-8	7.597 E-8	1.743 E-7	1.692 E-7
TOTAL	4.214 E-7	2.460 E-7	8.340 E-7	8.583 E-7
Fraction in group 15 ($1.35 \leq E \leq 2.47$ MeV)	6%	5%	23%	11%
Fraction in thermal group (group 25)	23%	31%	21%	20%

Table 10. Gamma Spectra in Different Zones

(γ/cm^2/D-D fusion/group)

Energy Group	Zone 1	Zone 6	Zone 7	Zone 10
1	0	0	0	0
2	0	1.354 E-10	0	9.514 E-11
3	4.410 E-9	2.150 E-9	1.246 E-8	1.111 E-9
4	7.889 E-9	8.458 E-10	8.792 E-9	3.639 E-8
5	1.134 E-9	2.286 E-9	7.931 E-10	5.222 E-9
6	1.611 E-9	0	1.692 E-9	2.667 E-9
7	3.889 E-9	2.604 E-9	6.125 E-9	1.259 E-8
8	1.210 E-9	5.806 E-10	3.118 E-9	3.736 E-9
9	5.250 E-12	3.813 E-10	1.036 E-8	2.752 E-9
10	1.242 E-9	5.125 E-10	8.417 E-9	8.076 E-9
11	1.199 E-9	7.730 E-9	2.453 E-9	1.508 E-9
12	2.861 E-9	1.040 E-9	5.375 E-9	8.731 E-9
13	1.341 E-9	9.083 E-10	1.181 E-9	8.410 E-9
14	2.870 E-9	8.563 E-9	5.097 E-9	1.826 E-9
15	5.792 E-9	1.407 E-8	1.830 E-8	3.048 E-8
16	7.778 E-9	2.826 E-9	8.889 E-9	1.410 E-8
17	2.458 E-9	1.615 E-9	1.128 E-8	4.257 E-9
18	5.007 E-8	5.243 E-8	3.860 E-7	9.563 E-8
19	4.417 E-8	2.521 E-8	6.389 E-8	7.750 E-8
20	3.250 E-8	2.806 E-8	6.132 E-8	6.076 E-8
21	3.172 E-9	1.581 E-10	1.281 E-9	4.201 E-10
TOTAL	1.756 E-7	1.522 E-7	6.165 E-7	3.762 E-7
Fraction in Groups 18 - 21 (E < 1 MeV)	74%	70%	83%	63%

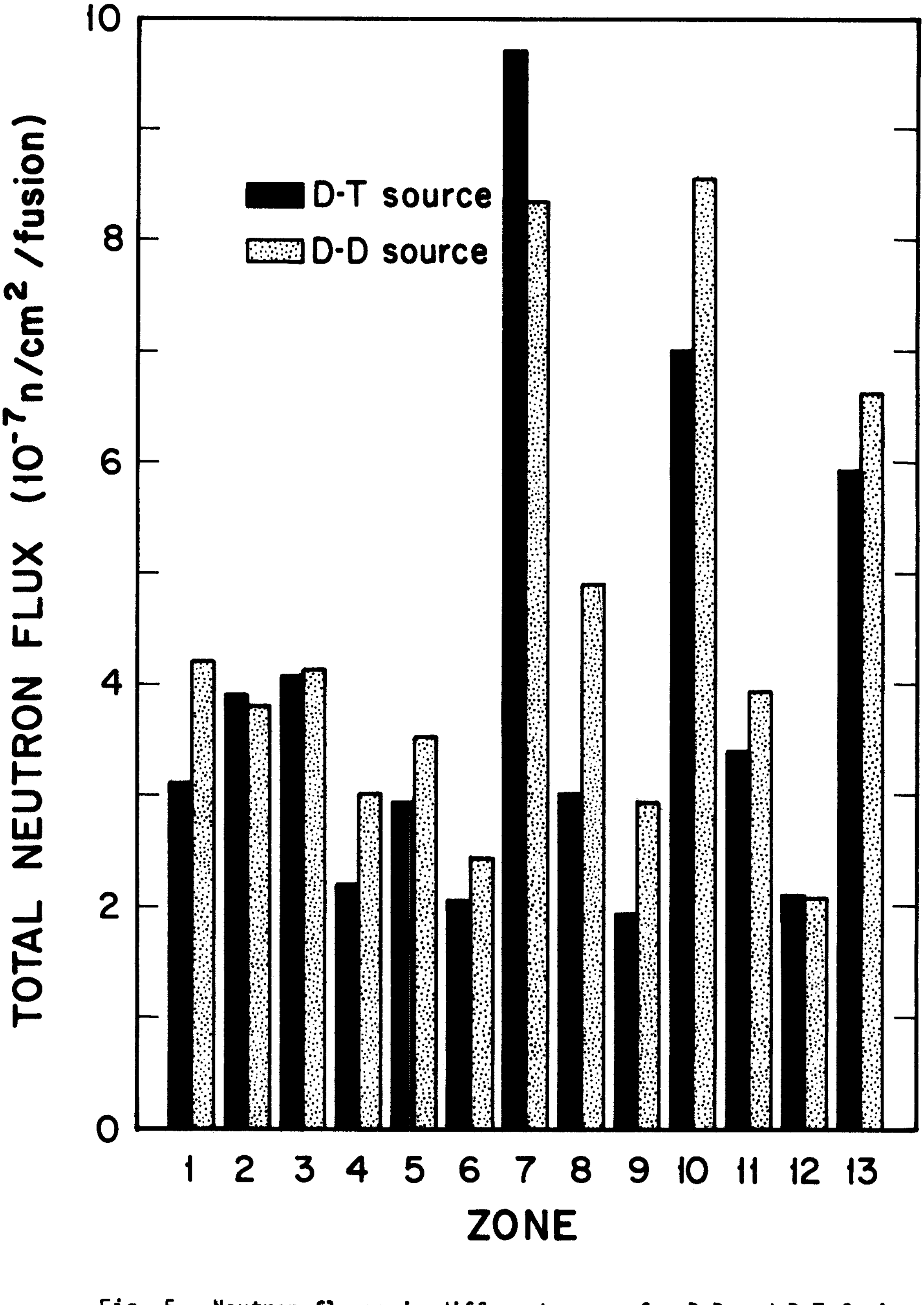

Fig. 5. Neutron fluxes in different zones for D-D and D-T fusion.

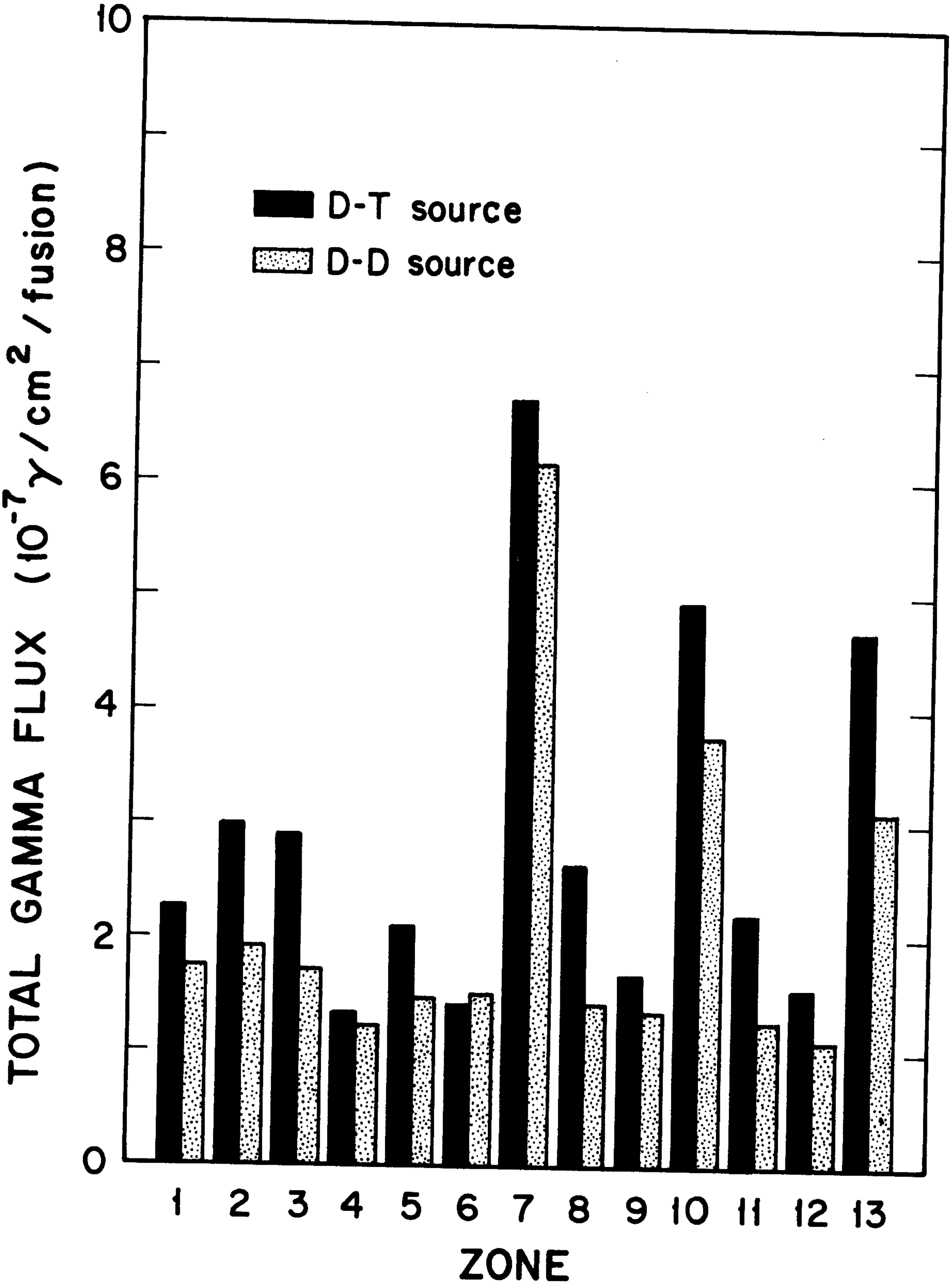

Fig. 6. Gamma fluxes in different zones for D-D and D-T fusion.

finite width and the fact that neutrons are scattered (mostly by elastic scattering) rather than being absorbed. Eighty percent of the neutrons interacting with the steel will remain in the same source group. The flux in the source group in zone 7 is larger than that predicted by $1/4\pi R^2$ (1.304×10^{-7}) due to the abovementioned reasons and the fact that neutrons scattered in the different regions will be bouncing between the basement walls and contributing to the flux in zone 7. The gamma spectrum is slightly harder than that in the D-T case because of the harder spectrum of gamma photons produced by lower energy neutrons in H_2O. However, a softer spectrum is obtained in zone 7 as lower energy neutrons produce softer gamma spectra in steel.

IV. Summary

Three-dimensional coupled neutronics-photonics calculations have been performed for PBFA-II. The accelerator tank, the target chamber, the upper shield tank and the basement area with surrounding concrete and soil were included in the model. Volume detectors were used at different locations in the basement representative of possible locations for the laser triggering systems. The effect of elevation above the basement floor was investigated. Calculations were performed for both cases of D-T and D-D fusion neutrons. The neutron and gamma spectra were calculated at the different locations. The largest neutron and gamma fluxes occur at the proposed location for the splitter table. More than 85% of the neutrons are at energies below 1.35 MeV for all proposed locations for the YAG and KrF lasers. More than 70% of the gamma photons have energies below 1 MeV at these locations. The results of this work can be used to calculate the absorbed dose in the different laser triggering systems and other sensitive diagnostic equipment.

Acknowledgement

Funding for this work was provided by the Sandia National Laboratories, Albuquerque, New Mexico.

References

1. G. Yonas, Proc. of U.S. - Japan Seminar on Theory and Application of Multiple Ionized Plasmas Produced by Laser and Particle Beams, May 3-7, 1982, Nara, Japan.

2. RSIC Code Package CCC-203, "MORSE-CG," Radiation Shielding Information Center, Oak Ridge National Laboratory (1977).

3. RSIC Data Library Collection, "VITAMIN-C, 171 Neutron, 36 Gamma-Ray Group Cross Sections Library in AMPX Interface Format for Fusion Neutronics Studies," DLC-41, Oak Ridge National Laboratory (1979).

4. M.E. Sawan, W.F. Vogelsang and D.K. Sze, "Radiation Shielding of Heavy Ion Beam Focussing Magnets in HIBALL," UWFDM-438, University of Wisconsin (1981).